A novel model for evaluating dynamic thermal comfort under demand response events

Marika Vellei, Jérôme Le Dréau

A novel model for evaluating dynamic thermal comfort under demand response events

Marika Vellei[a,*], Jérôme Le Dréau[a]

[a] *LaSIE - Laboratoire des Sciences de l'Ingénieur pour l'Environnement (UMR CNRS 7356)*
La Rochelle University, 23 Avenue Albert Einstein, 17000 La Rochelle

**corresponding author: marika.vellei@univ-lr.fr*

Abstract

Smart thermostats are expected to become the first residential appliance to offer significant demand response (DR) capacity worldwide. Their success will depend, to a large extent, on how people's thermal comfort will be affected by the dynamic conditions induced during DR events. To study and evaluate such conditions, researchers have so far mainly relied on Fanger's predicted mean vote (PMV) and predicted percentage of dissatisfied (PPD) indices. However, Fanger's model is only suited to predict PMV and PPD under steady-state or slowly changing environmental conditions. For the comfort evaluation of transient thermal conditions, there is still a limited understanding of the psycho-physiological phenomena of thermal alliesthesia and thermal habituation/adaptation, which govern the dynamic thermal perception. In this paper, these two phenomena are incorporated, for the first time, into a dynamic thermal comfort model, which is able to predict the percentage of dissatisfied occupants from Fanger's PMV index. The novel PPD is the result of both a static (PMV-based) and a transient (hedonic and adaptive) component. Since the model builds on the widely-used PMV index, it has the potential to be largely adopted by academics and practitioners and greatly improve their understanding of how people experience comfort and discomfort under DR-induced dynamic environments.

Keywords

space heating and cooling, demand response, dynamic thermal comfort, thermal alliesthesia, thermal habituation/adaptation

1. Introduction

1.1. Context

Flexibility in electric power consumption can be inexpensively and efficiently secured via demand response (DR), which can be defined as *"a concept describing an incentivizing of customers by costs, ecological information or others in order to initiate a change in their consumption or feed-in pattern"* [1]. In buildings, DR-activated smart thermostats typically induce cyclical set-point modulations, which are characterized by repeated rises and falls of the indoor temperature. For example, the French company Voltalis in coordination with RTE has already tested on 45000 French households different DR events, under the form of successions of 10-minutes off periods of the heating system and periods of rest (on) of 20 minutes [2]. The magnitude of the induced rates of temperature change depends on several factors, such as the thermal characteristics of the buildings and the types of emitters and controllers used. To evaluate thermal comfort under such a variety of dynamic thermal environments, researchers have so far mainly used Fanger's traditional PMV/PPD model [3–10]. However, Fanger's model is derived from a steady-state heat balance equation and steady-state laboratory experiments [11] and is, therefore, only suited to predict thermal comfort under steady-state or slowly changing (rate of temperature change less than 2°C/h) indoor conditions [12]. Thus, Fanger's model is not able to correctly predict PPD for rates of temperature change higher than 2°C/h, which is most often the case during DR events, especially in buildings with a low-performance thermal envelope.

1.2. Literature

Current standards only offer indications on the maximum temperature changes allowed over certain periods. The ASHRAE Standard 55 [13] sets to 2.2°C/h the maximum temperature change allowed for ramps or drifts during exposures of 1h. Ramps refer to actively controlled changes, drifts to passive (free-running) changes. Cyclical temperature variations with periods longer than 15 minutes are treated as ramps or drifts. For cyclical variations with periods shorter than 15 minutes a maximum peak-to-peak variation of 1.1°C is allowed. The ISO standard 7730 [14] sets a maximum peak-to-peak variation of 1°C for cyclic variations and recommends to use steady-state evaluation methods for ramps and drifts if the rate of temperature change is less than 2°C/h.

In the last 20 years, thermal comfort research has been dominated by the paradigm of adaptive thermal comfort [15,16]. The adaptive thermal comfort model has revolutionized the way of evaluating thermal comfort in naturally ventilated buildings by demonstrating that people's thermal preferences track seasonal temperature variations. In practice, the model prescribes comfort temperature boundaries - function of the external air temperatures - within which the indoor temperature can fluctuate. Hence, the adaptive theory acknowledges people's adaptation to diurnal and seasonal temperature fluctuations and justifies it in terms of physiological, psychological and behavioural changes. However, it does not explain how short-term temperature fluctuations affect occupants' thermal comfort.

The majority of the laboratory experiments investigating transient thermal environments deals with step-change conditions [17–25]. While these studies give valuable insights into the process of dynamic thermal perception, they are more useful to model dynamic thermal comfort in transitional spaces than during DR events. In fact, exposures to cyclical temperature changes elicit phenomena that cannot be observed during single step-change exposures (see, for example, thermal habituation/adaptation in Section 2.3). During the Seventies and the Eighties few laboratory investigations have studied both cyclical and monotonic temperature variations [26–28] but they gave a mixed picture and did not clearly show whether dynamic conditions extend or shrink the steady-state comfort zone. By reviewing them, Hensen concluded that for rates below 1.5°C/h there is not a significant decrease or increase of Fanger's steady-state comfort zone [29].

More recent research on cyclical and monotonic temperature variations narrows down to 4 laboratory experiments [30–33], which are mainly addressing summer conditions. Of these, three studies [30–32] deal with cyclical temperature variations and one [33] focuses on ramps. The studied rates of temperature change are mostly below 6°C/h, only the work of Zhang [31] deals with rates of temperature change up to 30°C/h. The results of these recent studies indicate that cyclical changes in temperature might have a favourable impact on occupants' thermal comfort, even under the high rates of temperature change studied in Zhang's experiment [31]. In fact, none of the cycles tested in Zhang's experiment complied with the ASHRAE standard, yet half of them were found to be thermally acceptable, showing that the ASHRAE limits are overly conservatives. Furthermore, Fanger's PMV/PPD model was found to predict a tighter comfort range than the one actually observed during the studied modulations [31].

As an alternative to Fanger's steady-state heat balance model, more complex multi-segmental dynamic models of human thermoregulation have been developed in the past 40 years [34,35]. They simulate the physical interaction between a dynamic indoor environment and an occupant and predict high-resolution skin and body core temperatures. The predicted temperatures can then be used as inputs of physiologically-based thermal perception models [36–40], which are built by means of regression analysis of experimental thermal sensation and/or comfort votes and simulated or monitored physiological parameters. Most of these models predict the dynamic thermal sensation of the whole-body under uniform indoor environments. Only the model of Zhang [37–39] predicts both local and whole-body thermal sensation and comfort under both uniform and non-uniform indoor environments.

1.3. Research aims

Despite the considerable efforts put into the advancement of these physiologically-based thermal perception models, a poor knowledge of the processes driving dynamic thermal perception still limits their further development. In particular, the two phenomena of thermal alliesthesia and thermal habituation/adaptation, which are known to affect the dynamic thermal perception, have so far received little consideration. In this paper, we include these two phenomena into a novel dynamic PPD index, which is derived from regression analysis of recently-collected experimental data [31]. We take a completely different approach than the one currently adopted by physiologically-based models since we assume that the brain can anticipate the PMV-based thermal perception and modify it with hedonic and adaptive attributes. This is based on the anticipatory comfort responses observed during step-change temperature variations [17–25]. Hence, the novel PPD combines both a static (PMV-based) and a transient (hedonic and adaptive) component. Since the novel model builds on the widely-used PMV index, it has the potential to be largely adopted by academics and practitioners and greatly improve their understanding of how people experience comfort and discomfort under cyclical temperature variations.

2. A new conceptual framework

2.1. Pathways for thermal perception

Thermal perception begins with the activation of cutaneous thermoreceptors, which are pseudo-unipolar primary sensory neurons with one branch ending in molecular temperature sensors (located in the peripheral tissues) and the other branch consisting of cell bodies (located, for most of the body, in the dorsal root ganglia). Primary sensory neurons convert thermal stimuli into electrical signals, which travel to second-order neurons in the dorsal horn of the spinal cord, where information is further processed before being transmitted to the central nervous system (Figure 1).

The molecular temperature sensors mostly belong to the family of the transient receptor potential (TRP) ion channels [41]. Depending on the type of TRP ion channel that they are expressing, primary sensory neurons can selectively encode heat and cold: TRPV1-expressing sensory neurons encode heat, while TRPM8-neurons encode cold [42]. Few TRPV1- and TRPM8-neurons encode both heat and cold. Second-order neurons in the dorsal horn of the spinal cord can also be classified based on their response to cold, heat and both heat and cold (Figure 1) [43].

The central nervous system includes:

- The preoptic area of the hypothalamus for the initiation of autonomic thermoregulatory processes (vasodilatation and vasoconstriction, sweating, shivering, etc.) [44].
- The primary somatosensory cortex and the thalamus which are believed to provide an objective assessment of temperature and form the basis of thermal sensation (feeling warm, neutral, cold, etc.) [44].
- The lateral parabrachial nucleus which is thought to play an hedonic role in thermal perception and form the basis of thermal comfort [45]. It is also thought that thermal comfort (and not thermal sensation) is important for activating behavioural thermoregulatory actions in humans [46]. Thermoregulatory behaviours have been defined as *"an attempt to avoid what humans call thermal discomfort or displeasure and to obtain thermal pleasure"* [47].

Hence, both thermal comfort and thermal sensation have their origins in the central nervous system. However, thermal comfort has a more hedonic origin than thermal sensation [46]. Thus, by predicting occupants' thermal sensation we are only capturing the objective part of thermal perception, overlooking its hedonic component, which becomes particularly important during transient conditions [22,29,48]. For this reason, this paper focuses on predicting occupants' dissatisfaction rather than their thermal sensation. Throughout this article, the terms *"thermal comfort"* and *"thermal satisfaction"* are used interchangeably to indicate the hedonic component of thermal perception.

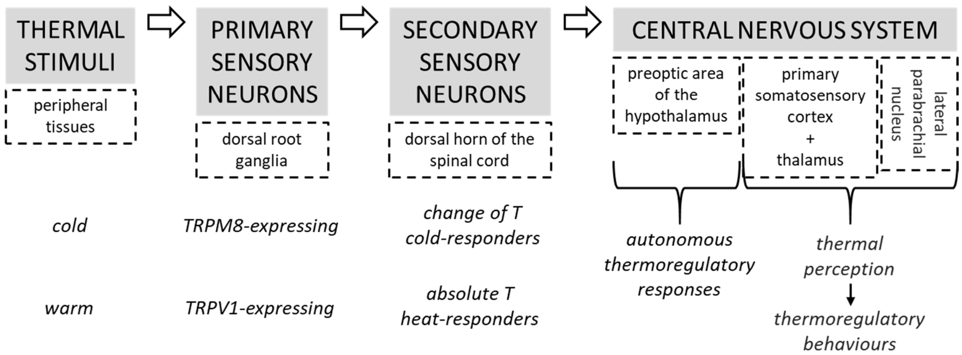

Figure 1 Pathways for autonomous thermoregulatory responses and thermal perception

2.2. Thermal alliesthesia

According to Cabanan, alliesthesia is *"the property of a given stimulus to arouse pleasure or displeasure according to the internal state of the subject"* [49]. For the particular case of thermal alliesthesia, any thermal stimulus that minimizes the thermoregulatory load error is perceived as pleasant, while any stimulus that exacerbates it is perceived as unpleasant. When a stimulus is perceived as pleasant this transient condition can be described with the term of positive alliesthesia. On the contrary, a condition characterized by a transient unpleasant stimulus can be indicated as negative alliesthesia. Pleasure is also a sign of the usefulness of a stimulus since not-useful unpleasant stimuli are drivers of thermoregulatory behaviours [29,46,47,49].

Occupants can experience alliesthesia when undergoing a variation of any environmental or personal variable influencing thermal comfort. Under the transient conditions induced by DR events occupants typically stay within the thermal neutral zone (TNZ) of vasomotor regulation, which is characterized by adjustments of skin blood flow (i.e. vasodilatation and vasoconstriction). In this zone, the concept of spatial alliesthesia, firstly discovered by Marks and Gonzalez [48] and subsequently formalized by Parkinson and de Dear [50], becomes of great relevance since the body core temperature stays invariant while the different regional skin temperatures displaced from their set-points are responsible for the thermoregulatory load-error. Thus, for the case of spatial thermal alliesthesia, the thermoregulatory load-error emanates from cutaneous thermoreceptors distributed throughout the entire body [50], while the more conventional notion of alliesthesia considers that pleasure is driven from load errors emanating from the body core [49]. In the rest of this paper the general term *"alliesthesia"* is used to indicate the phenomenon of spatial thermal alliesthesia.

The intensity of the alliesthesial effect is driven by both the magnitude of the load error (i.e. the physiological state of the occupant away from the neutral condition) and the rate of change in the skin temperature [51]. It is not clear if the intensity of the alliesthesial effect is equally affected by cooling and warming rates of the skin. Recent research evidence from neuroscience experiments shows that, in the dorsal horn of the spinal cord, the temperature intensity-response relationships in the cold and heat ranges are different [43]. The response of cold-sensitive spinal neurons has been shown to mainly depend on the rate of cooling and rapidly adapt. In contrast, heat-sensitive spinal neurons are found to mainly respond to the absolute temperatures and not adapt. Since the spinal cord is the first relay centre in which peripheral thermal stimuli are processed before being sent to the central nervous system (Figure 1 in Section 2.1), these results suggest that humans are more sensitive to cooling than warming and that cooling rates of the skin might elicit stronger alliesthesial effects compared to warming rates. However, this has not been confirmed yet.

2.3. Thermal habituation/adaptation

During repeated thermal exposures, adaptive processes acting at either peripheral or central level can modify occupants' thermal perception. Habituation is a form of nonassociative learning, which happens in the central nervous system, while sensory adaptation (or sensory fatigue) is directly related to the activity of primary sensory neurons. They both lead to a reduction of the normal response or sensation and both have been shown to be reversible [52]. Hence, if the stimulus is withheld for a period of time after habituation/adaptation and then given again, the response will become again normal. In this paper we do not distinguish between habituation and adaptation and refer to both of them with the general term of *"habituation/adaptation"*. Habituation/adaptation has been observed in several thermal comfort laboratory experiments [53–56] and is believed to depend on modifications of the way thermal stimuli are processed, with repeated stimulation of the synapses causing changes in the magnitude of the postsynaptic responses to subsequent stimulations [57,58].

We know that thermal habituation/adaptation develops over a much shorter time scale than physiological adaptation and anticipates any morphological, chemical, functional, and genetic changes that reduce physiological strain when exposed to thermal stress [59,60]. However, little is yet known on how adaptive processes influence thermal comfort, particularly during cyclical temperature variations. Most of the insights on these adaptive processes remain limited to research on thermal pain perception [61,62].

3. Methods

3.1. Dataset

For developing the novel PPD model, we used experimental data collected at the Indoor Environmental Quality Laboratory of the University of Sydney as part of a study investigating the comfort impact of DR events [31]. We decided to focus solely on this data for two main reasons:

- Among the recent literature of dynamic thermal comfort studies, this is the laboratory experiment employing the greatest number of participants exposed to the highest rates of temperature change (up to 30°C/h).
- The studied temperature variations correspond to those normally found during summer DR events in university lecture theatres and, being cyclical, allow to investigate the phenomena of thermal habituation/adaptation.

As part of Zhang's experiment, fifty-six students were exposed to 6 different cyclical temperature variations, with each variation having an overall duration of 2 hours, see Figure 2. The study was conducted in summer and was specifically addressing an air-conditioning (cooling) case. The students were wearing a standardized clothing ensemble whose clothing insulation was estimated to be 0.5 clo, including the insulation of the chair. The experimental sessions were characterized by adapting temperatures (i.e. the temperature to which the skin is adapted for half hour before the temperature variation starts) of 22°C (conditions no. 2, 3 and 4 in Figure 2) and 24°C (conditions no. 5, 6 and 7 in Figure 2). Air and globe temperature, relative humidity and air velocity were measured every 5 minutes over the 2 hours of each of the 6 studied conditions. Thermal acceptability was also monitored every 5 minutes for each participating subject.

In Figure 2, the observed percentage of dissatisfied subjects, *observed* PD, is interpreted from a binary thermal acceptability scale and is defined as the ratio of thermal unacceptability votes to total votes. Figure 2 also shows the operative temperature T_{op} (on the left) and Fanger's PPD (on the right). It is worth noting that Fanger's PPD index is derived using a different definition for the percentage of dissatisfied subjects, which is the percent of people voting above warm or below cool (≥2 or ≤-2) on the 7-point ASHRAE thermal sensation scale. This method of derivation of PPD is suitable under steady-state conditions. However, under dynamic conditions, warm and cold thermal sensations can be associated with pleasure if positive alliesthesia is elicited, hence Fanger's derivation of the PPD index can correctly predict thermal dissatisfaction only under steady-state conditions.

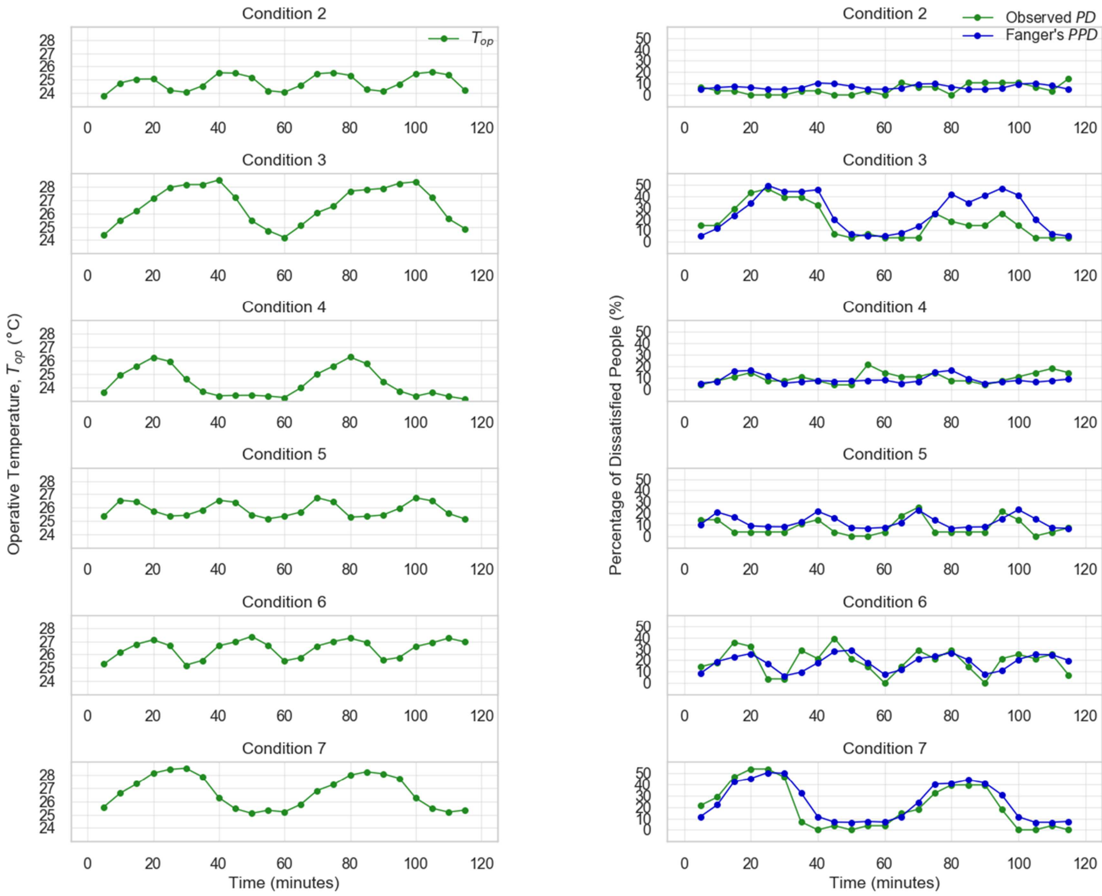

Figure 2 Operative temperature (T_{op}, left) and percentage of dissatisfied people (observed PD and Fanger's PPD, right) for the 6 cyclical temperature variations (conditions 2-7). The observed PD represents the vote of all participating students every 5 minutes, while T_{op} corresponds to the mean calculated value every 5 minutes. Adapted from [31].

3.2. Statistical analysis

Multiple linear regression with possible third-way interactions is used to model the relationship between the independent or explanatory variables (described in Section 3.3) and the response variable (the observed PD). Multiple linear regression is implemented in Python using the function *statsmodels.api.ols()*. Backward elimination is used for selecting the *"best"* subset of predictors in Section 4.1. To evaluate the predictive performance of the selected statistical model, cross-validation is used in Section 4.2.

3.3. Predictors

Fanger's PMV index integrates the effect of all six basic thermal comfort parameters: air temperature, mean radiant temperature, air movement, humidity, clothing insulation and metabolic heat generated by human activity. According to Fanger, the body heat balance is a necessary but not sufficient condition to achieve thermal comfort since it is also necessary to have a mean skin temperature and a sweat secretion rate within comfort limits which depend on the metabolic activity and are determined from steady-state experiments in climate chambers [11]. Bearing in mind that the PMV does not represent the actual thermal sensation under dynamic thermal conditions, it is worth stressing that our main interest here is to develop a statistical model to predict thermal comfort rather than thermal sensation. Hence, we use the PMV index as an indicator of the body's steady-state thermal condition. In doing so, we assume that the brain can anticipate the PMV-based thermal perception. This also allows to define the novel PPD directly from Fanger's PMV index. Since the relation between PMV and PD is not linear, we use as predictor the exponential function directly derived by Fanger based on laboratory experiments involving 1300 subjects:

$$ePMV = e^{\left(-0.03353PMV^4 - 0.2179PMV^2\right)} \quad 1)$$

To include the phenomenon of alliesthesia (Section 2.2), a categorical independent variable, called $alliesthesia$, is introduced. $positive$ and $negative$ alliesthesial states are defined based on the rate of change or gradient of PMV. Here, we use a second-order central finite difference method to estimate $\frac{\partial PMV}{\partial t}$, which is sampled every 5 minutes and is expressed in *vote/h*. On the warm side of the TNZ (PMV>0), $negative\ alliesthesia$ occurs when $\frac{\partial PMV}{\partial t}$ is positive, i.e. when the occupant is moving away from a PMV equal to zero (thus inducing or exacerbating the thermal stress). On the contrary, $positive\ alliesthesia$ occurs when $\frac{\partial PMV}{\partial t}$ is negative, i.e. when the occupant is moving towards a neutral PMV (thus relieving or removing the thermal stress). On the cold side of the TNZ, the opposite applies.

To further characterize the phenomenon of alliesthesia, we introduce a continuous independent variable, the absolute value of $\frac{\partial PMV}{\partial t}$, which measures the intensity of the alliesthesial effect at each thermal state and accounts for the fact that skin thermoreceptors respond not only to the temperature but also to the rate of temperature change [29]. $\left|\frac{\partial PMV}{\partial t}\right|$ includes the variation of any thermal parameter. In this study, the air temperature is mainly varied (as it is most often the case during DR events) and, therefore, $\left|\frac{\partial PMV}{\partial t}\right|$ is strongly correlated to the rate of temperature change.

If the thermal state stays unchanged or changes very slowly neither an alliesthesial pleasant sensation nor an unpleasant one arises. To model this state we set the additional level of $no\ alliesthesia$ for $\left|\frac{\partial PMV}{\partial t}\right| < 1\ vote/h$. 1 *vote/h* corresponds to a rate of change of the operative temperature of about 3°C/h, the other conditions (clothing, activity, air velocity and air humidity) being constant. Thus, $alliesthesia$ is a factor with three possible levels: $positive$, $negative$ and no (Figure 3).

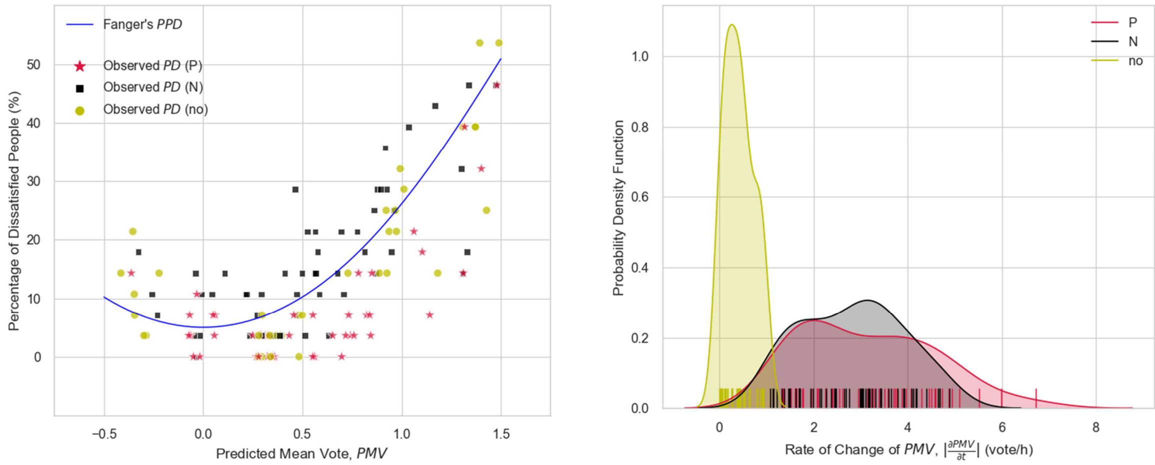

Figure 3 On the left: Observed PD as a function of PMV for the three levels of positive (P), negative (N) and no alliesthesia in red, black and yellow respectively. Fanger's PPD model is plotted in blue for purposes of comparison. On the right: Gaussian kernel density estimate of the absolute values of the rate of change of PMV.

The phenomenon of thermal habituation/adaptation (Section 2.3) is modelled by introducing a predictor, called $exposure$, which is defined as the sum, at each cycle, of the squared difference between the actual PMV and the minimum PMV_{min} during the cycle:

$$exposure = \sum_{cycle} (PMV - PMV_{min})^2 dt \ [discomfort^2 \ minutes] \qquad 2)$$

Where:

dt = duration of the thermal stimulus [minutes].

PMV_{min} = minimum PMV reached at each cycle, which is equal to 0 if the PMV gets negative.

The calculated PMV and $exposure$ for the 6 cyclical temperature variations are shown in the left and right of Figure 4 respectively.

The selected independent or explanatory variables ($ePMV$, $alliesthesia$, $\left|\frac{\partial PMV}{\partial t}\right|$ and $exposure$) are calculated every 5 minutes from the aggregated data of all the participants. The makes a total of 138 data points to derive the model.

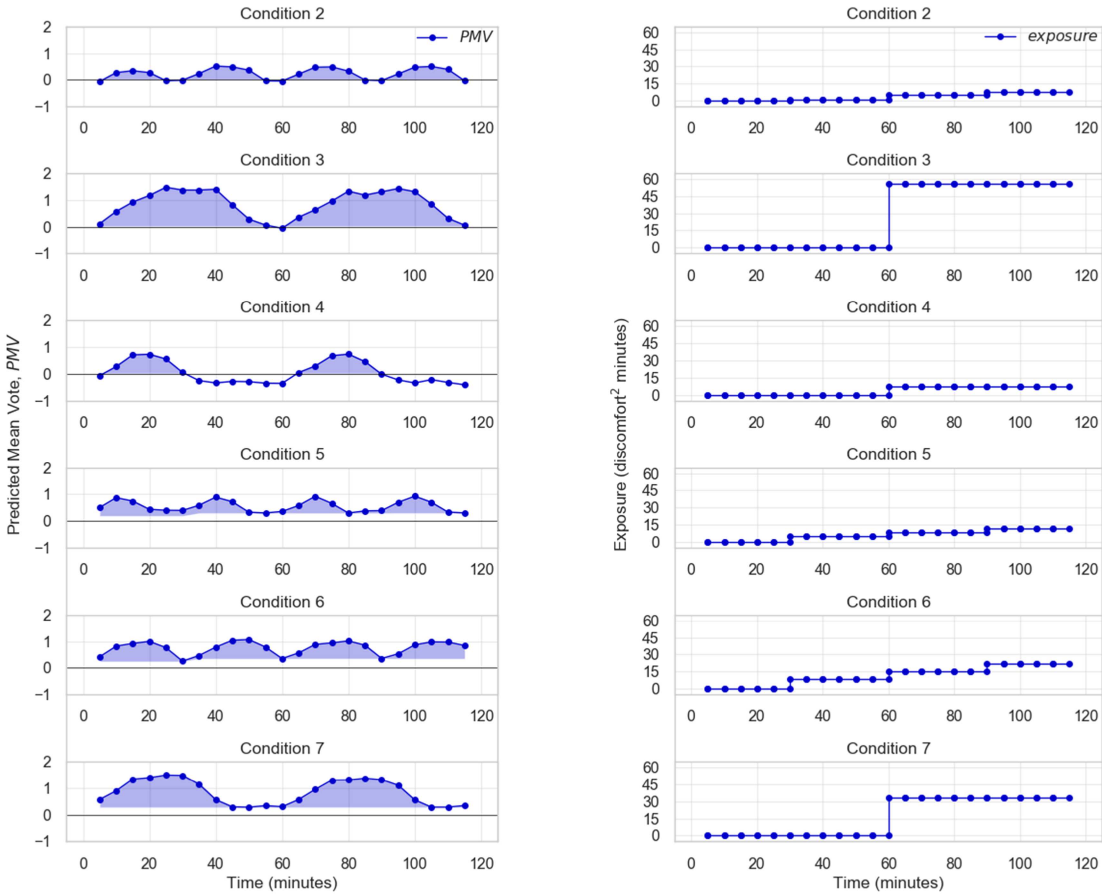

Figure 4 Calculated PMV (left) and $exposure$ (right) for the 6 cyclical temperature variations (conditions 2-7).

4. Results

4.1. Backward elimination

Backward elimination starts with all of the predictors in the model and consists in refitting the model several times, each time removing the least significant term (with the largest p-value over 0.01), until left with only significant effects. Significant effects have p-value smaller than 0.01.

The resulting model has a coefficient of determination R^2 equal to 0.836, hence our predictors explain 83.6% of the variability of our dependent variable, the observed PD. The $\mathrm{F-ratio}$ is equal to 48.67 and the p-value associated with the model as a whole is very small, $\mathrm{p} < 2.51e^{-42}$, which means that the regression model is a good fit of the data. The key assumptions of linear regression (normality, homoscedasticity and no autocorrelation of the residual errors, no multicollinearity of the independent variables) have been met. Regression coefficients of the resulting linear model are shown in Table 1.

There is one main significant predictor, $ePMV$, and 4 significant interaction terms: $alliesthesia * \left|\frac{\partial PMV}{\partial t}\right|$, $alliesthesia * \left|\frac{\partial PMV}{\partial t}\right| * ePMV$, $alliesthesia * exposure$, $alliesthesia * exposure * ePMV$. It is to be noticed that we have included only the interaction terms as the main effects were not significant. This was taken into account in the interpretation of the interaction terms given below.

The fact that the coefficient of $ePMV$ is negative means that: the higher the values of $ePMV$, the lower the percentage of dissatisfied people (PD). Since $ePMV$ is given by Equation 1, higher values of $ePMV$ implies lower values of PMV. Thus, we can conclude that: the lower the values of PMV (in absolute terms), the lower the percentage of dissatisfied people (PD). The first significant interaction term ($alliesthesia * \left|\frac{\partial PMV}{\partial t}\right|$) means that effect of $\left|\frac{\partial PMV}{\partial t}\right|$ differs across the different levels of $alliesthesia$: $\left|\frac{\partial PMV}{\partial t}\right|$ has significant effect in the $positive\ alliesthesia$ level but its effect is not significant in the $negative$ and no levels of $alliesthesia$. For the first time, we observe that the intensity of positive alliesthesia is significantly affected by the magnitude of the cooling rate. The second significant interaction term ($alliesthesia * \left|\frac{\partial PMV}{\partial t}\right| * ePMV$) means that the interaction between $\left|\frac{\partial PMV}{\partial t}\right|$ and $ePMV$ is positive and significant only for the $positive\ alliesthesia$ level, i.e. the effect of $\left|\frac{\partial PMV}{\partial t}\right|$ becomes stronger as we go further from the neutrality. The third significant interaction term ($alliesthesia * exposure$) means that the effect of $exposure$ varies among the different levels of $alliesthesia$: $exposure$ has significant effect in the $negative$ level but its effect is not significant in the $positive$ and no levels of $alliesthesia$. Finally, the fourth significant interaction term ($alliesthesia * exposure * ePMV$) means that the interaction between $exposure$ and $ePMV$ is positive and significant only for the $negative\ alliesthesia$ level, i.e. the effect of $exposure$ is larger as we go further from the neutrality.

Table 1 Regression coefficients for the predictors. Significant terms are indicated with an asterisk.

	Estimate	Std. Error	t	Significance p
$Intercept$	100.3416	8.726	11.499	0.000*
$ePMV$	-96.9343	9.596	-10.101	0.000*
$alliesthesia[N] * \left\|\frac{\partial PMV}{\partial t}\right\|$	4.6839	3.946	1.187	0.237
$alliesthesia[P] * \left\|\frac{\partial PMV}{\partial t}\right\|$	-10.5864	3.372	-3.139	0.002*
$alliesthesia[no] * \left\|\frac{\partial PMV}{\partial t}\right\|$	19.1658	16.932	1.132	0.260
$alliesthesia[N] * \left\|\frac{\partial PMV}{\partial t}\right\| * ePMV$	-3.3458	4.309	-0.777	0.439
$alliesthesia[P] * \left\|\frac{\partial PMV}{\partial t}\right\| * ePMV$	10.1192	3.771	2.683	0.008*
$alliesthesia[no] * \left\|\frac{\partial PMV}{\partial t}\right\| * ePMV$	-20.5624	19.788	-1.039	0.301
$alliesthesia[N] * exposure$	-1.1778	0.256	-4.607	0.000*
$alliesthesia[P] * exposure$	-0.1667	0.287	-0.581	0.563
$alliesthesia[no] * exposure$	-0.6990	0.290	-2.409	0.017
$alliesthesia[N] * exposure * ePMV$	1.1679	0.315	3.711	0.000*
$alliesthesia[P] * exposure * ePMV$	0.1403	0.326	0.430	0.668
$alliesthesia[no] * exposure * ePMV$	0.6553	0.383	1.711	0.090

The novel model for predicting PPD on the warm side of the TNZ (95% of the available experimental data comes from the warm side of the TNZ) takes the form:

$$Novel\ PPD = 100.34 + \left(a * \left|\frac{\partial PMV}{\partial t}\right| + b * exposure - 96.93\right) * e^{(-0.03*PMV^4 - 0.23*PMV^2)} + c * \left|\frac{\partial PMV}{\partial t}\right| + d * exposure \quad 3)$$

Where:

- a=10.12h, b=0.14min^{-1}, c=-10.59h, d=-0.17min^{-1} for $positive\ alliesthesia$,
- a=-3.34h, b=1.17min^{-1}, c=4.68h, d=-1.18min^{-1} for $negative\ alliesthesia$,
- a=-20.56h, b=0.65min^{-1}, c=19.16h, d=-0.7min^{-1} for $no\ alliesthesia$.

4.2. Cross-validation

Obtaining high R^2 values does not necessarily imply having a good model. It is easy to over-fit the data by including too many degrees of freedom and inflating R^2. Thus, to further evaluate the predictive performance of the derived statistical model, cross-validation is used. The dataset is split 10 times into 3 different training and validation/test sets, equal or close in size. The training set is used to train the model, and the validation/test set is used to validate the model on data that it has never seen before. The root-mean-square-error (RMSE) is used to measure the predictive accuracy of each model.

$$\text{RMSE} = \sqrt{\frac{\sum(PD - PPD)^2}{n}} \quad 4)$$

Where PD is the observed value, PPD is the predicted value and n is the number of data points.

Figure 5 shows the boxplots of the RMSE calculated for four different models: the first model has only $ePMV$ as predictor (1 predictor), the second model has $ePMV$, $alliesthesia$, $\left|\frac{\partial PMV}{\partial t}\right|$ and $exposure$ as predictors (4 predictors without any interaction term), the third model is the model that we have just derived with the significant interaction terms (5 predictors), the last model includes all the possible third-way interactions between $ePMV$, $alliesthesia$, $\left|\frac{\partial PMV}{\partial t}\right|$ and $exposure$ (14 predictors). From Figure 5 we can see that our model (5 predictors) has the smaller mean RMSE, which is less than 6%. This corresponds to a percentage decrease of the mean RMSE of about 30% compared to Fanger's RMSE, which is calculated using the entire dataset and shown with the red dashed line in Figure 5.

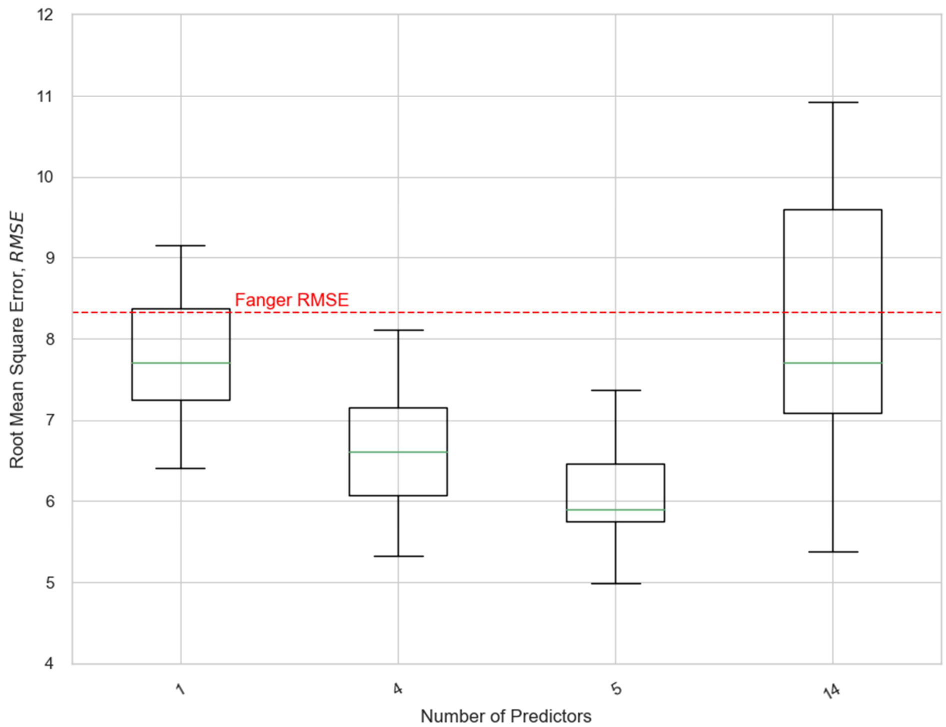

Figure 5 Boxplots of the RMSEs associated to the four different models tested. Fanger's RMSE is calculated using the entire dataset and is shown with the red dashed line.

5. Discussion

The novel PPD model is represented in Figure 6 for different values of $\left|\frac{\partial PMV}{\partial t}\right|$ and $exposure$ and for the range of PMV values studied in Zhang's experiment. Validity of the model beyond that range is discussed in the following paragraph. From Figure 6 we can notice that for $exposure$ equal to $0\, discomfort^{\,2}\, minutes$ and $\left|\frac{\partial PMV}{\partial t}\right|$ less than $1\, vote/h$ (i.e. no alliesthesia in yellow) there is neither alliesthesia nor habituation/adaptation and, thus, the new model nearly coincides with Fanger's model. Also, in the case of positive alliesthesia and for a thermal environment that is rapidly changing (high rates of change of PMV), the predicted percentage of dissatisfied occupants is less than 5%, which is the minimum value obtainable using Fanger's PPD model, and reaches up to 0%. This aligns well with the hypothesis of alliesthesia: *"higher levels of occupant satisfaction in transient or textured thermal environments may be explained by the hedonic overtones from the alliesthesial effect"* [63]. Figure 7 show the predictions of the novel model compared to Fanger's PPD values over the used dataset.

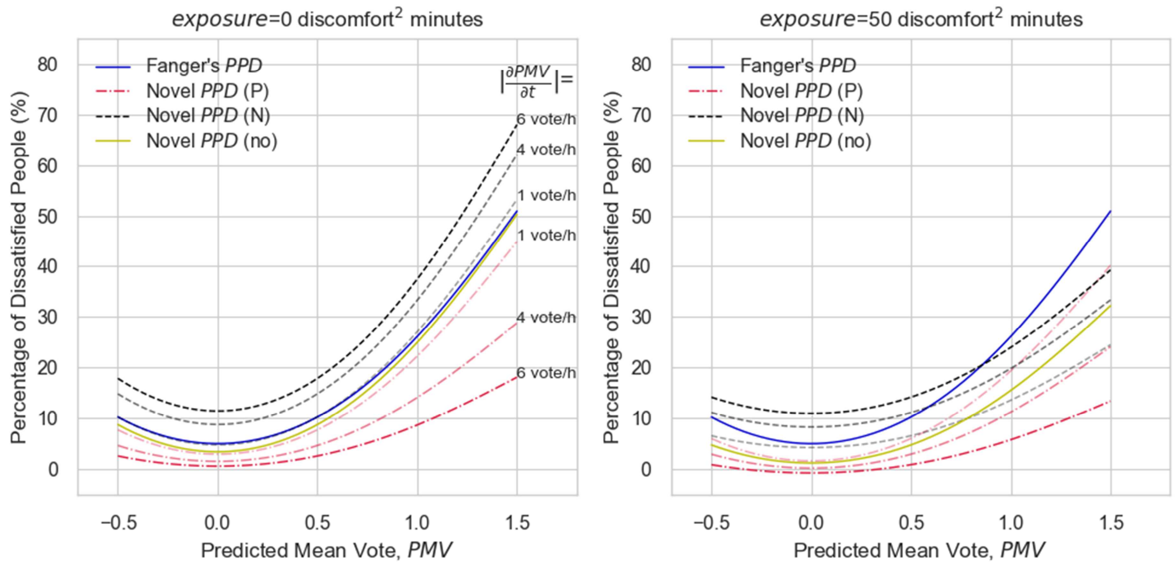

Figure 6 Predicted percentage of dissatisfied occupants as a function of PMV at different combinations of $exposure$ (0 and 50 discomfort^2 minutes) and $\left|\frac{\partial PMV}{\partial t}\right|$ (1, 4 and 6 vote/h) for the cases of positive (red), negative (black) and no (yellow) $alliesthesia$. Fanger's PPD is plotted in blue for purposes of comparison.

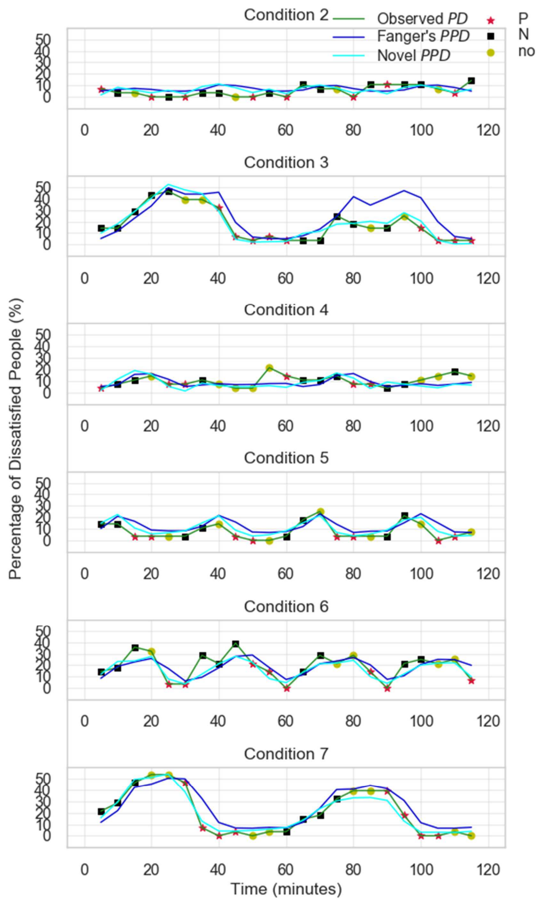

Figure 7 Percentage of dissatisfied people (observed PD, Fanger's PPD and Novel PPD) for the 6 cyclical temperature variations (conditions 2-7). The three levels of positive (P), negative (N) and no alliesthesia are highlighted in red, black and yellow respectively.

The recent discovery, anticipated in Section 2.2, of cold-sensitive spinal neurons mainly responding to the rate of temperature change and heat-sensitive spinal neurons mainly responding to the absolute temperature [43] can be directly linked to our results from the warm side of the TNZ, which show a significant effect of the rate of temperature change, i.e. $\left|\frac{\partial PMV}{\partial t}\right|$, only during the cooling down phases of positive alliesthesia (see upper part of Figure 8). This means that humans are more sensitive to cooling than warming and that the intensity of the alliesthesial effect depends on the rate of cooling but does not depend on the rate of warming. This recent discovery also explains the much larger thermal sensation overshoots observed during temperature down-step changes than during temperature up-step changes [17–19].

On the warm side of the TNZ cooling is related to positive alliesthesia, while on the cold side of the TNZ cooling is associated with negative alliesthesia (Figure 8). Thus, we can hypothesize that, on the cold side of the TNZ, $\left|\frac{\partial PMV}{\partial t}\right|$ has a significant effect only during the cooling down phase of negative alliesthesia and we can assume that this effect has the same magnitude as the positive alliesthesial effect on the warm side. On the basis of these hypotheses, we can extend the model to the cold side of the TNZ zone as shown in Figure 9.

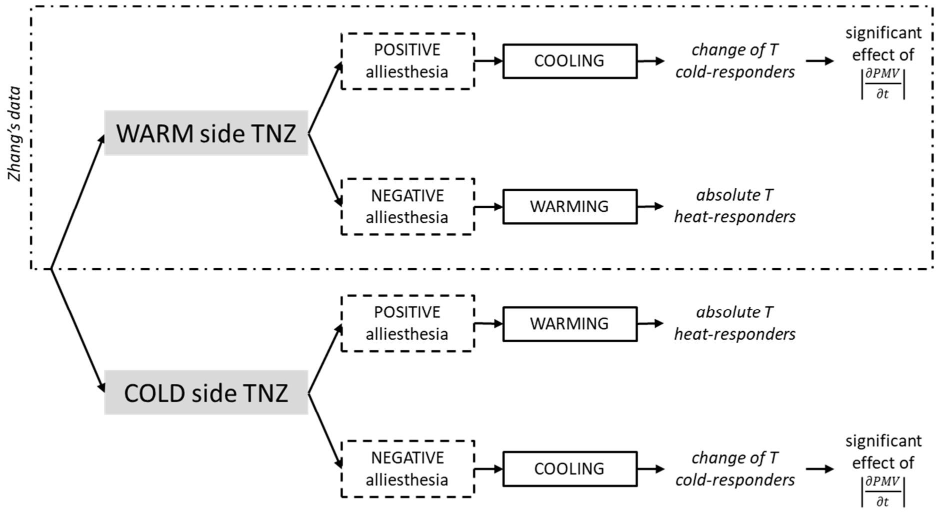

Figure 8 Asymmetric alliesthesial effect on the warm and cold side of the TNZ.

From Figure 9 we can observe that, on the warm side of the TNZ, the thermal comfort zone extends when the cooling rates are faster, while, on the cold side of the TNZ, the thermal comfort zone has the opposite behaviour and shrinks as the temperature decreases faster. This asymmetric behaviour has important implications for the way in which set-point modulations are implemented during DR events. In summer, it is important to have modulations characterized by rapid cooling phases, while in winter the greatest attention should be given to minimize cooling rates to avoid eliciting uncomfortable negative alliesthesial effects.

According to the ASHRAE standard [13], a thermal environment can be regarded as acceptable if more than 80% of the occupants find it thermally acceptable. In Figure 9 the 80% acceptable limit on the warm side of the TNZ extends up to a PMV of 1.5, which is almost the double of Fanger's limit of about 0.85. While, on the cold side of the TNZ, it shrinks down to a PMV of 0.5. Hence, the magnitude of the error between the novel model and Fanger's model depends on the rate of temperature change. Higher rates of temperature change imply greater differences between the two models.

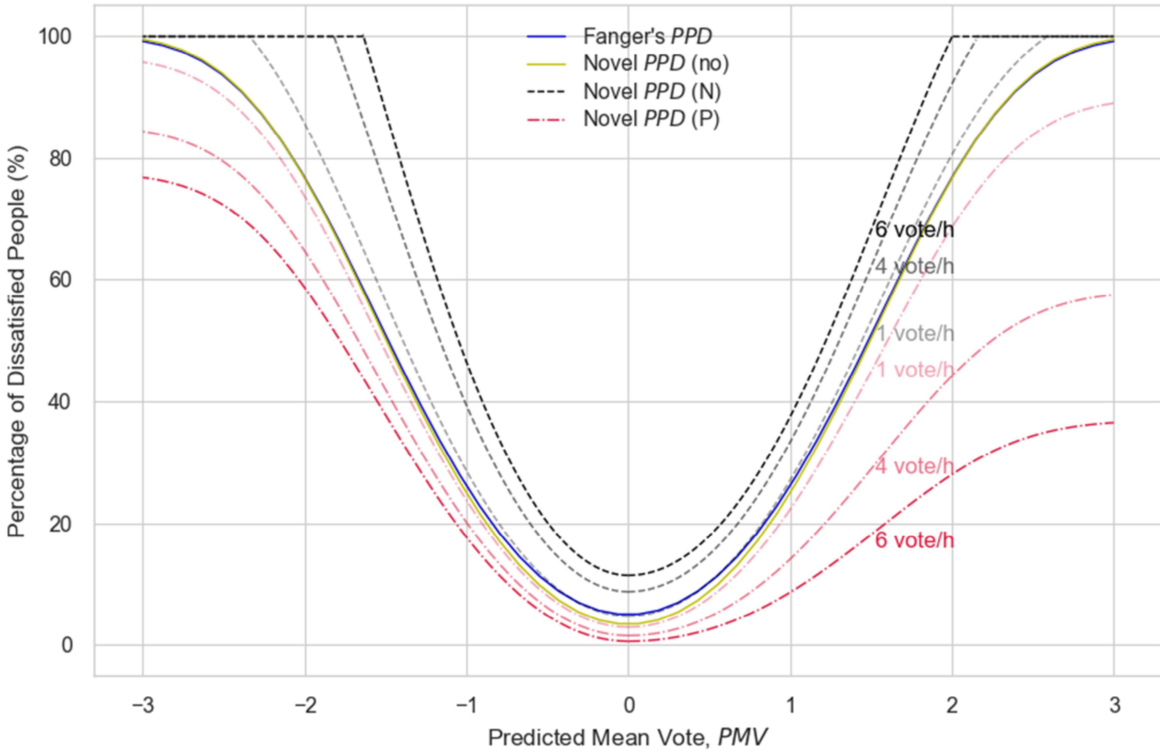

Figure 9 Extended novel PPD model for $exposure$ *equal to* $0\ discomfort^2\ minutes.$

6. Limitations and future directions

The results presented herein suggest that accounting for the phenomena of thermal alliesthesia and thermal habituation/adaptation by using the novel PPD model allows to improve the accuracy of Fanger's PPD index. However, there are still some important limitations, which are outlined below.

In deriving this model we have assumed that the brain can anticipate the PMV-based thermal perception and modify it with hedonic and adaptive attributes. A part of the variance of PD is explained by the anticipatory response; the rest is explained by a transient (hedonic and adaptive) component. This is an oversimplified model of how the brain integrates and elaborates signals from cutaneous thermoreceptors. This oversimplification forcedly implies a loss of accuracy but the final model has the advantage of being relatively simple to understand and easy to apply. A more accurate approach would be to develop a novel physiological-based thermal perception model which can properly account for thermal alliesthesia and thermal habituation/adaptation. This could be a future direction to take.

Additionally, only 5% of the available data comes from the cold side of the TNZ; hence, we can only speculate about what it is happening on that side. Further experimental studies collecting data from the cold side of the TNZ are needed to confirm the hypothesized behaviour. The cold side is as important as the warm side for studying DR, especially in European countries. Thus, giving answers to this question is of main importance. Also, data from the warm side of the TNZ are limited to PMV lower than 1.5; more data collected from PMV higher than 1.5 could make the model robust over the whole range of PMV values.

The results from this paper only apply to uniform thermal environments. However, positive thermal alliesthesia has also been observed in non-uniform thermal environments, when local body parts are cooled or heated to relieve whole-body discomfort [53,54].

Finally, we do not know how thermal habituation/adaptation evolves during periods longer than 2 hours and if, for example, a plateau of minimum discomfort is reached after multiple repeated stimulations. New laboratory experiments characterized by periods longer than 2 hours are needed to better understand the phenomenon of thermal habituation/adaptation. Furthermore, we ignore if and how the shape of the temperature variation influences thermal habituation/adaptation and we do not know for how long thermal habituation/adaptation lasts. The available knowledge on the subject is still very scarce, and comes mostly from research on thermal pain perception. New thermal comfort laboratory experiments are needed to fill these gaps.

7. Conclusions

This paper presents a novel dynamic thermal comfort model, which can be used to predict, under the transient indoor conditions induced by DR events, the percentage of dissatisfied people from Fanger's PMV index. The new PPD index is derived from data collected in a laboratory experiment and allows a percentage decrease of the mean RMSE of about 30% compared to Fanger's PPD index over the used dataset. Overall, the magnitude of the error between the novel model and Fanger's model depends on the rate of temperature change. Higher rates of temperature change imply greater prediction differences between the two models.

The new modelling approach includes the two psycho-physiological phenomena of thermal alliesthesia and thermal habituation/adaptation and contributes to a better understanding of their impact on dynamic thermal perception. For the first time we show that:

- Positive alliesthesia on the warm side of the TNZ is highly sensitive to the cooling rate, in contrast to negative alliesthesia which is shown to not depend on the rate of temperature increase. This is explained, at cellular level, by the fact that the response of cold-sensitive spinal neurons is mainly a function of the rate of cooling, while heat-sensitive spinal neurons respond to absolute temperatures.
- Thermal habituation/adaptation can significantly reduce thermal discomfort in the case of negative alliesthesial stimuli.

The novel PPD model can be used to evaluate occupant's thermal dissatisfaction under different types of simulated set-point modulations and have the potential to inform the way temperature modulations are controlled during DR events. As an example, in summer, it is important to have modulations characterized by rapid cooling phases to elicit comfortable positive alliesthesial effects. Also, these findings open up new interesting directions of research in the field of dynamic thermal comfort.

Acknowledgements

This research was funded by the French National Research Agency (ANR-17-CE22-0005-01). We thank Dr Fan Zhang, Professor Richard de Dear and Dr Christina Candido for making the aggregated data of their laboratory experiment available. We also thank the anonymous Reviewers for their useful comments and Professor Christian Inard for the valuable discussions.

References

[1] CEN-CENELEC-ETSI, Smart Grid Coordination Group – Sustainable Processes, 2012.

[2] RTE, Évaluation des économies d'énergie et des effects de bord associés aux effacements de consommation, 2016.

[3] D. Da Silva, Analyse de la flexibilité des usages électriques résidentiels : application aux usages thermiques, École Nationale Supérieure des Mines de Paris, 2011.

[4] M.-A. Leduc, A. Daoud, C. Le Bel, Developing winter residential demand response strategies for electric space heating, in: BS2011 12th Conf. Int. Build. Perform. Simul. Assoc., Sydney (AU), 2011.

[5] P. Morales-Valdés, A. Flores-Tlacuahuac, V.M. Zavala, Analyzing the effects of comfort relaxation on energy demand flexibility of buildings: A multiobjective optimization approach, Energy Build. 85 (2014) 416–426. doi:10.1016/j.enbuild.2014.09.040.

[6] J. Le Dréau, P. Heiselberg, Energy flexibility of residential buildings using short term heat storage in the thermal mass, Energy. 111 (2016) 991–1002. doi:10.1016/j.energy.2016.05.076.

[7] G. Masy, E. Georges, C. Verhelst, V. Lemort, P. André, Smart grid energy flexible buildings through the use of heat pumps and building thermal mass as energy storage in the Belgian context, Sci. Technol. Built Environ. 21 (2015) 800–811. doi:10.1080/23744731.2015.1035590.

[8] T.Q. Péan, J. Ortiz, J. Salom, Impact of Demand-Side Management on Thermal Comfort and Energy Costs in a Residential nZEB, Buildings. 7 (2017).

[9] T. Weiß, A.M. Fulterer, A. Knotzer, Energy flexibility of domestic thermal loads – a building typology approach of the residential building stock in Austria, Adv. Build. Energy Res. (2017) 1–16. doi:10.1080/17512549.2017.1420606.

[10] S. Agapoff, M. Jandon, T. Guiot, Impact of a tariff based heating load control on energy, comfort and environment : a parametric study in residential and office buildings, in: Int. SEEDS Conf. 2017 Sustain. Ecol. Eng. Des. Soc., Leeds (UK), 2017.

[11] P.O. Fanger, Thermal comfort: analysis and applications in environmental engineering, McGraw-Hill, 1972.

[12] B. Koelblen, A. Psikuta, A. Bogdan, S. Annaheim, R.M. Rossi, Thermal sensation models: Validation and sensitivity towards thermo-physiological parameters, Build. Environ. 130 (2018) 200–211. doi:10.1016/j.buildenv.2017.12.020.

[13] ASHRAE, ANSI/ASHRAE Standard 55-2017 - Thermal Environmental Conditions for Human Occupancy, 2017.

[14] ISO, Ergonomics of the thermal environment - Analytical determination and interpretation of thermal comfort using calculation of the PMV and PPD indices and local thermal comfort criteria (ISO 7730 - 2005), 2005.

[15] J.F. Nicol, M.A. Humphreys, Thermal comfort as part of a self-regulating system, Build. Res. Pract. 1 (1973) 174–179. doi:10.1080/09613217308550237.

[16] R.J. de Dear, G.S. Brager, Developing an adaptive model of thermal comfort and preference, ASHRAE Trans. 104 (1998) 145–167.

[17] R.J. de Dear, J.W. Ring, P.O. Fanger, Thermal Sensations Resulting From Sudden Ambient Temperature Changes, Indoor Air. 3 (1993) 181–192. doi:10.1111/j.1600-0668.1993.t01-1-00004.x.

[18] W. Ji, B. Cao, Y. Geng, Y. Zhu, B. Lin, Study on human skin temperature and thermal evaluation in step change conditions: From non-neutrality to neutrality, Energy Build.

156 (2017) 29–39. doi:10.1016/j.enbuild.2017.09.037.

[19] H. Liu, J. Liao, D. Yang, X. Du, P. Hu, Y. Yang, B. Li, The response of human thermal perception and skin temperature to step-change transient thermal environments, Build. Environ. 73 (2013) 232–238. doi:10.1016/j.buildenv.2013.12.007.

[20] W. Ji, B. Cao, M. Luo, Y. Zhu, Influence of short-term thermal experience on thermal comfort evaluations: A climate chamber experiment, Build. Environ. 114 (2017) 246–256. doi:10.1016/j.buildenv.2016.12.021.

[21] J. Xiong, Z. Lian, X. Zhou, J. You, Y. Lin, Potential indicators for the effect of temperature steps on human health and thermal comfort, Energy Build. 113 (2016) 87–98. doi:10.1016/j.enbuild.2015.12.031.

[22] A.P. Gagge, J.A.J. Stolwijk, J.D. Hardy, Comfort and thermal sensations and associated physiological responses at various ambient temperatures, Environ. Res. 1 (1967) 1–20. doi:https://doi.org/10.1016/0013-9351(67)90002-3.

[23] X. Du, B. Li, H. Liu, D. Yang, W. Yu, J. Liao, Z. Huang, K. Xia, The Response of Human Thermal Sensation and Its Prediction to Temperature Step-Change (Cool-Neutral-Cool), PLoS One. 9 (2014) e104320. doi:10.1371/journal.pone.0104320.

[24] Y. Zhang, J. Zhang, H. Chen, X. Du, Q. Meng, Effects of step changes of temperature and humidity on human responses of people in hot-humid area of China, Build. Environ. 80 (2014) 174–183. doi:10.1016/j.buildenv.2014.05.023.

[25] Z. Zhang, Y. Zhang, E. Ding, Acceptable temperature steps for transitional spaces in the hot-humid area of China, Build. Environ. 121 (2017) 190–199. doi:10.1016/j.buildenv.2017.05.026.

[26] D.P. Wyon, T. Asgeirsdottir, P. Kjerulf-Jensen, P.O. Fanger, The effects of ambient temperature swings on comfort, performance and behaviour, Arch. Sci. Physiol. (Paris). 27 (1973) 441–458.

[27] F.H. Rohles, G.A. Milliken, D.E. Skipton, I. Krstic, Thermal comfort during cyclical temperature fluctuations, ASHRAE Trans. 86 (1980) 125–140.

[28] L.G. Berglund, R.R. Gonzalez, Occupant acceptability of eight-hour-long temperature ramps in the summer at low and high humidities, ASHRAE Trans. 84 (1978) 278–284.

[29] J.L.M. Hensen, Literature review on thermal comfort in transient conditions, Build. Environ. 25 (1990) 309–316. doi:10.1016/0360-1323(90)90004-B.

[30] M. Miura, T. Ikaga, Human response to the indoor environment under fluctuating temperature, Sci. Technol. Built Environ. (2016). doi:10.1080/23744731.2016.1184550.

[31] F. Zhang, R. de Dear, C. Candido, Thermal comfort during temperature cycles induced by direct load control strategies of peak electricity demand management, Build. Environ. 103 (2016) 9–20. doi:10.1016/j.buildenv.2016.03.020.

[32] L. Schellen, W.D. van Marken Lichtenbelt, M.G.L.C. Loomans, J. Toftum, M.H. de Wit, Differences between young adults and elderly in thermal comfort, productivity, and thermal physiology in response to a moderate temperature drift and a steady-state condition., Indoor Air. 20 (2010) 273–283. doi:10.1111/j.1600-0668.2010.00657.x.

[33] J. Kolarik, J. Toftum, B.W. Olesen, A. Shitzer, Occupant Responses and Office Work Performance in Environments with Moderately Drifting Operative Temperatures (RP-1269), HVAC&R Res. 15 (2009) 931–960. doi:10.1080/10789669.2009.10390873.

[34] D. Fiala, K.J. Lomas, M. Stohrer, Computer prediction of human thermoregulatory and temperature responses to a wide range of environmental conditions, Int. J. Biometeorol. 45 (2001) 143–159. doi:10.1007/s004840100099.

[35] D. Fiala, G. Havenith, P. Bröde, B. Kampmann, G. Jendritzky, UTCI-Fiala multi-node model of human heat transfer and temperature regulation, Int. J. Biometeorol. 56 (2012) 429–441. doi:10.1007/s00484-011-0424-7.

[36] D. Fiala, K.J. Lomas, M. Stohrer, First principles modeling of thermal sensation responses in steady-state and transient conditions, in: ASHRAE Trans., 2003: pp. 179–186. doi:10.1590/S1517-83822008000200021.

[37] H. Zhang, E. Arens, C. Huizenga, T. Han, Thermal sensation and comfort models for non-uniform and transient environments, part III: Whole-body sensation and comfort, Build. Environ. 45 (2010) 399–410. doi:10.1016/j.buildenv.2009.06.020.

[38] H. Zhang, E. Arens, C. Huizenga, T. Han, Thermal sensation and comfort models for non-uniform and transient environments, part II: Local comfort of individual body parts, Build. Environ. 45 (2010) 389–398. doi:10.1016/j.buildenv.2009.06.015.

[39] H. Zhang, E. Arens, C. Huizenga, T. Han, Thermal sensation and comfort models for non-uniform and transient environments: Part I: Local sensation of individual body parts, Build. Environ. 45 (2010) 380–388. doi:10.1016/j.buildenv.2009.06.018.

[40] S. Takada, S. Matsumoto, T. Matsushita, Prediction of whole-body thermal sensation in the non-steady state based on skin temperature, Build. Environ. 68 (2013) 123–133. doi:10.1016/j.buildenv.2013.06.004.

[41] J. Vriens, B. Nilius, T. Voets, Peripheral thermosensation in mammals, Nat. Rev. Neurosci. (2014). doi:10.1038/nrn3784.

[42] D.A. Yarmolinsky, Y. Peng, L.A. Pogorzala, M. Rutlin, M.A. Hoon, C.S. Zuker, Coding and Plasticity in the Mammalian Thermosensory System, Neuron. 92 (2016) 1079–1092. doi:10.1016/j.neuron.2016.10.021.

[43] C. Ran, M.A. Hoon, X. Chen, The coding of cutaneous temperature in the spinal cord, Nat. Neurosci. 19 (2016) 1201–1209. doi:10.1038/nn.4350.

[44] H.J. Solinski, M.A. Hoon, Cells and circuits for thermosensation in mammals, Neurosci. Lett. 690 (2019) 167–170. doi:10.1016/j.neulet.2018.10.026.

[45] M.L. Kringelbach, K.C. Berridge, Pleasures of the Brain, Oxford University Press, 2009.

[46] K. Nagashima, K. Tokizawa, S. Marui, Chapter 15: Thermal comfort, Handb. Clin. Neurol. 156 (2018).

[47] M. Cabanac, P. Serres, Peripheral heat as a reward for heart rate response in the curarized rat, J. Comp. Physiol. Psychol. 90 (1976) 435–441. doi:10.1037/h0077213.

[48] L.E. Marks, R.R. Gonzalez, Skin temperature modifies the pleasantness of thermal stimuli, Nature. 247 (1974) 473–475. doi:10.1038/247473a0.

[49] M. Cabanac, Sensory Pleasure, Q. Rev. Biol. 54 (1979) 1–29. doi:10.1086/410981.

[50] T. Parkinson, R. de Dear, Thermal pleasure in built environments: physiology of alliesthesia, Build. Res. Inf. 43 (2015) 288–301. doi:10.1080/09613218.2015.989662.

[51] T. Parkinson, R. De Dear, C. Candido, Thermal pleasure in built environments: Alliesthesia in different thermoregulatory zones, Build. Res. Inf. 44 (2016) 20–33. doi:10.1080/09613218.2015.1059653.

[52] C.H. Rankin, T. Abrams, R.J. Barry, S. Bhatnagar, D.F. Clayton, J. Colombo, G. Coppola,

M.A. Geyer, D.L. Glanzman, S. Marsland, F.K. McSweeney, D.A. Wilson, C.F. Wu, R.F. Thompson, Habituation revisited: An updated and revised description of the behavioral characteristics of habituation, Neurobiol. Learn. Mem. 92 (2009) 135–138. doi:10.1016/j.nlm.2008.09.012.

[53] E. Arens, H. Zhang, C. Huizenga, Partial- and whole-body thermal sensation and comfort - Part I: Uniform environmental conditions, J. Therm. Biol. 31 (2006) 53–59. doi:10.1016/j.jtherbio.2005.11.028.

[54] E. Arens, H. Zhang, C. Huizenga, Partial- and whole-body thermal sensation and comfort - Part II: Non-uniform environmental conditions, J. Therm. Biol. 31 (2006) 60–66. doi:10.1016/j.jtherbio.2005.11.027.

[55] T. Parkinson, R. de Dear, Thermal pleasure in built environments: spatial alliesthesia from air movement, Build. Res. Inf. 45 (2017) 320–335. doi:10.1080/09613218.2016.1140932.

[56] J.C. Stevens, S.S. Stevens, Warmth and cold: Dynamics of sensory intensity, J. Exp. Psychol. 60 (1960) 183–192. doi:10.1037/h0040840.

[57] L.E. Armstrong, J. Stoppani, Central nervous system control of heat acclimation adaptations: An emerging paradigm, Rev. Neurosci. 13 (2002) 271–285. doi:10.1515/REVNEURO.2002.13.3.271.

[58] S.G. Solomon, A. Kohn, Moving Sensory Adaptation beyond Suppressive Effects in Single Neurons, Curr. Biol. 24 (2014). doi:10.1016/j.cub.2014.09.001.

[59] N.A.S. Taylor, Human heat adaptation, Compr. Physiol. (2014). doi:10.1002/cphy.c130022.

[60] H.A.M. Daanen, W.D. Van Marken Lichtenbelt, Human whole body cold adaptation, Temperature. (2016). doi:10.1080/23328940.2015.1135688.

[61] M. Jepma, M. Jones, T.D. Wager, The dynamics of pain: Evidence for simultaneous site-specific habituation and site-nonspecific sensitization in thermal pain, J. Pain. 15 (2014) 734–746. doi:10.1016/j.jpain.2014.02.010.

[62] M. Hollins, D. Harper, W. Maixner, Changes in pain from a repetitive thermal stimulus: The roles of adaptation and sensitization, Pain. 152 (2011) 1583–1590. doi:10.1016/j.pain.2011.02.049.

[63] T. Parkinson, R. de Dear, C. Candido, Perception of Transient Thermal Environments: Pleasure and Alliesthesia, in: 7th Wind. Conf. Chang. Context Comf. an Unpredictable World, Windsor (UK), 2012.